

Universal behaviour of α -viscosity in black hole accretion discs

Marek A. Abramowicz^{1,2,3*}, Axel Brandenburg^{4,5}, Jiří Horák⁶, Debora Lančová^{2,3**},
 John C. Miller^{7,8}, Ewa Szuszkiewicz⁹, and Maciek Wielgus¹⁰

¹ Physics Department, Gothenburg University, SE-412-96 Göteborg, Sweden

² Nicolaus Copernicus Astronomical Center, Polish Academy of Sciences, Bartycka 18, PL-00-716 Warszawa, Poland

³ Research Center for Computational Physics and Data Processing, Institute of Physics, Silesian University in Opava, Bezručovo nám. 13, CZ-746 01 Opava, Czech Republic

⁴ Nordita, Hannes Alfvéns väg 12, SE-106 91 Stockholm, Sweden

⁵ The Oskar Klein Centre, Department of Astronomy, Stockholm University, AlbaNova, 10691 Stockholm, Sweden

⁶ Astronomical Institute of the Academy of Sciences, Boční II 1401/1a, CZ-141 31 Praha 4, Czech Republic

⁷ Department of Physics (Astrophysics), University of Oxford, Keble Road, Oxford, OX1 3RH, United Kingdom

⁸ International School for Advanced Studies, SISSA, Via Bonomea 265, 34136 Trieste, Italy

⁹ Institute of Physics and CASA*, University of Szczecin, ul. Wielkopolska 15, PL-70-451 Szczecin, Poland

¹⁰ Instituto de Astrofísica de Andalucía-CSIC, Glorieta de la Astronomía s/n, E-18008 Granada, Spain

Received ???; accepted ???

ABSTRACT

The Shakura-Sunyaev α -viscosity coefficient, defined as the ratio of total stress to total pressure, $\alpha = \mathbb{T}/p$, played an important role in the development of the accretion disc theory in the early 1970s. The origin of turbulence that causes the stress \mathbb{T} was unknown at that time. Shakura and Sunyaev assumed $\alpha = \text{const}$. Today we know that this was not quite realistic — the modern general relativistic magneto-hydrodynamic simulations (GRMHD) of black hole accretion discs revealed that α changes by about an order of magnitude within the disc, being smaller far away from the black hole and larger in the plunging region close in. It was found that the behaviour of α reflects some underlying, fundamental properties of the stress \mathbb{T} itself. In particular, as argued by several authors, the stress must be zero at the black hole horizon. We notice that the stress calculated in GRMHD simulations by different authors, including us, has a maximum rather close to the location of the circular photon orbit. We propose a formula that accurately describes this universal behaviour of α in terms of the “gyration radius”, a physical characteristic of rotation well known in Newtonian dynamics and in the black hole case uniquely defined by the Kerr space-time geometry. Analytic and semi-analytic models of black hole accretion discs provide an invaluable insight into fundamental physics, and the GRMHD simulations do not aspire to replace them. Rather, simulations could help to improve analytic models by making them more realistic. For example, our α -formula, deduced from the GRMHD simulations, may be handy in the construction of improved versions of thin and slim disc models.

Key words. black hole physics – turbulence – accretion, accretion disks – magnetohydrodynamics (MHD)

1. Motivation

The classic, analytic model by [Shakura & Sunyaev \(1973\)](#) is today still one of the pillars on which our understanding of the fundamental physics governing black hole accretion discs rests. The remarkable practical usefulness of the model results from its sharp clarity that was achieved by several brilliant assumptions that have been made. Perhaps the most important of them is the treatment of the “viscous” stress \mathbb{T} that powers the accretion disc’s radiation by enhancing angular momentum transport and dissipating orbital energy of matter into heat. Directly from the fundamental conservation laws, [Shakura & Sunyaev \(1973\)](#) derived equations for the radial fluxes of mass \dot{M} , angular

momentum \dot{J} , and energy \dot{E} in accretion discs:

$$\dot{M} = \int_{-H}^{+H} 2\pi r \rho v dz, \quad (1)$$

$$\dot{J} = \dot{M} j + \mathbb{T}, \quad \dot{E} = \dot{M} e + \Omega \mathbb{T}. \quad (2)$$

Here ρ is the mass density, v is the radial velocity of the matter, integration goes through the disc vertical thickness¹

$$z = H(r), \quad z = r \cos(\theta - \pi/2), \quad (3)$$

j and e are specific (per mass) angular momentum and energy, and Ω is the angular velocity. The difference $\Delta \dot{X}$ in

¹ For simplicity we consider here the Schwarzschild black hole and use spherical coordinates $\{t, r, \theta, \phi\}$ and metric signature $(+, -, -, -)$, in which $g_{tt} = c^2(1 - r_H/r)$ and $g_{\phi\phi} = -\sin^2(\theta) r^2$ with $r_H = 2GM/c^2$ being the horizon location and M being the mass of the black hole. The Kerr black hole formulae are given in the Appendix.

* e-mail: marek.abramowicz@physics.gu.se

** e-mail: debora.lancova@physics.cz

a flux \dot{X} between its radial locations r_1 and r_2 equals for the three fluxes (1), (2),

$$\Delta\dot{M} = 0, \quad \Delta\dot{J} = 0, \quad \Delta\dot{E} = \int_{r_2}^{r_1} F 2\pi r dr. \quad (4)$$

The radial flux of energy is not constant because energy is also partially radiated from the disc; F denotes the flux of energy that is locally radiated. From equations (1)–(4), [Shakura & Sunyaev \(1973\)](#) derived that the flux is given by

$$F = \frac{\dot{M}}{4\pi r} \left(\frac{d\Omega}{dr} \right) [j(r) - j_0], \quad (5)$$

where $j(r)$ is the radial angular momentum distribution in the disc and r_0 is the radial location of the place where the stress is zero, $\mathbb{T}(r_0) = 0$. Note that

$$j = \Omega(\tilde{r}^2) = \Omega \left(-\frac{g_{\phi\phi}}{g_{tt}} \right), \quad \tilde{r} = \text{gyration radius}. \quad (6)$$

Knowing r_0 and $j(r)$, and therefore also $\Omega(r)$, suffices to calculate the local radiation flux from equation (5).

For a razor thin disc $h = H/r \ll 1$, with accuracy to linear order terms $\mathcal{O}^1(h)$, one may assume

$$j(r) = \begin{cases} j_{\text{K}}(r) = \tilde{r}^2 \Omega_{\text{K}}(r) & \text{if } r > r_0 \\ j_{\text{K}}(r_0) = \text{const} & \text{if } r < r_0 \end{cases} \quad (7)$$

where $\Omega_{\text{K}}(r)$ is the Keplerian angular velocity and r_0 is the location of the innermost stable circular orbit (ISCO). Because $\Omega_{\text{K}}(r)$ and the location of the ISCO are known analytically in the Kerr geometry, from (7) one can derive the formula for the radiation flux emitted in an explicit (and very simple) form. Its Newtonian version reads

$$F(r) = \frac{3GM\dot{M}}{8\pi r^3} \left[1 - \sqrt{\frac{r_0}{r}} \right], \quad r_0 = \frac{6GM}{c^2}. \quad (8)$$

Formulae (5) and (8) are undoubtedly the most famous and useful in accretion disc theory. They have been used in Newtonian, Schwarzschild, and Kerr versions by numerous authors to calculate the observational appearance of accretion discs (e.g., [Novikov & Thorne 1973](#)). They do not depend on the stress \mathbb{T} and this was an enormous benefit in the early days of the development of the theory, when the nature of the stress was unknown. Because the stress enters a few other equations on which their model rests, [Shakura & Sunyaev \(1973\)](#) have adopted an ansatz known as the Shakura-Sunyaev viscosity prescription, which states that the stress is proportional to the total pressure,

$$\mathbb{T} = \alpha p, \quad \alpha = \text{const}. \quad (9)$$

There is a problem here. The formula (8) is valid only in the limit of a razor thin disc $h \rightarrow 0$, when only the lowest order ($\sim \mathcal{O}^1[h]$) terms are taken into account. When the disc luminosity is greater than about $\sim 0.3 L_{\text{Edd}}$, where L_{Edd} is the Eddington luminosity², several important physical effects, in particular radial advection of heat described by the $\mathcal{O}^2[h]$ terms, must be taken into account because they *qualitatively* change the physics of accretion. In particular, neither $j(r) = j_{\text{K}}(r)$ nor $\mathbb{T}(r_{\text{ISCO}}) = 0$ are valid.

² and corresponding mass accretion rate is $\dot{M}_{\text{Edd}} = L_{\text{Edd}}/(\eta c^2)$

The slim disc model ([Abramowicz et al. 1988](#)), comprehensively discussed by [Sądowski \(2009\)](#), incorporates all of the $\mathcal{O}^2[h]$ terms that are missed in the thin disc model. In slim discs the stress is zero not at the ISCO, but at the horizon r_{H} and, correspondingly, the constant $j_0 = j(r_0)$ that appears in (5) does not equal $j_{\text{K}}(r_{\text{ISCO}})$ as in thin discs, but instead is an eigenvalue of the problem, not known a priori. It cannot be assumed, but should be self-consistently calculated from the (extra) condition of regularity at the sonic radius r_{S} . The formula (5) only seemingly does not depend on the stress. In fact, when the terms $\mathcal{O}^2[h]$ are included, it depends strongly through the angular momentum distribution $j(r)$, which is directly governed by the stress. For this reason, in the plunging region of slim discs, that is located between the sonic radius and the horizon, $r_{\text{H}} < r < r_{\text{S}}$, the angular momentum is not constant and, correspondingly, the radiation flux $F(r)$ is not zero but may be quite large as calculations by [Sądowski \(2009\)](#) have clearly demonstrated. Obviously, the exact knowledge of the stress in the plunging region is important for calculating the radiation flux $F(r)$. Because slim disc models use the classic Shakura-Sunyaev ansatz for the stress (9), the currently used slim disc values of $F(r)$ are not realistic. A more realistic description of the stress in slim discs is needed.

2. Our α -prescription formula

We suggest that the Shakura-Sunyaev α -prescription formula (9) should be replaced by³

$$\alpha = \alpha(r) = \left[\alpha_P \left(\frac{r_{\text{H}}}{r} \right)^2 + \alpha_{\infty} \right] \left(1 - \frac{r_{\text{H}}}{r} \right). \quad (10)$$

By α_P and α_{∞} we denote two phenomenological constants: $\alpha_P = 4.71$ and $\alpha_{\infty} = 0.01$ give the best fit to the simulations by [Lančová et al. \(2019\)](#) denoted as **L19** in this work; see Figure 1.

The coordinate-independent version of (10), written with the help of the Killing vector η^ν (that describes the Schwarzschild metric time symmetry) and the Killing vector ξ^ν (axial symmetry) is⁴

$$\alpha = \alpha_P \left(\frac{r_{\text{H}}}{\tilde{r}} \right)^2 + \alpha_{\infty} (\eta\eta). \quad (11)$$

We use the notation $(\xi\xi) = \xi^\mu \xi^\nu g_{\mu\nu}$, and likewise for $(\eta\eta)$.

The “gyration radius” \tilde{r} is a key element in the arguments presented in this paper,

$$\tilde{r} = \left[-\frac{(\xi\xi)}{(\eta\eta)} \right]^{1/2}. \quad (12)$$

In Newtonian dynamics for a single particle orbiting a circle, the gyration radius is just the radius of the orbit, whilst for rotating solids, the gyration radius relates to the moments of inertia. [Abramowicz et al. \(1993\)](#) discussed in detail its physical meaning in Einstein’s General Relativity. As in Newtonian dynamics, in Einstein’s relativity for a particle with four-velocity u^ν in the Schwarzschild space-time, the specific angular momentum $j = -u_\phi/u_t$ and the angular velocity $\Omega = u^\phi/u^t = d\phi/dt$ are related by

$$j = \Omega \tilde{r}^2. \quad (13)$$

³ In the case of accretion discs around non rotating Schwarzschild black hole; see footnote 1.

⁴ In Appendix A, we give the Kerr metric formulae.

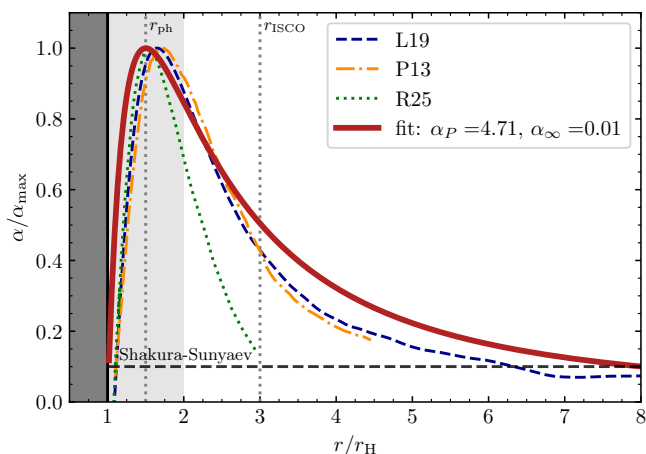


Fig. 1. The α -viscosity coefficient calculated in GRMHD simulations by [L19](#), [Penna et al. \(2013\)](#), denoted by [P13](#), and [Rule et al. \(2025\)](#), denoted by [R25](#), all for non-rotating black hole accretion discs, fitted to our α -prescription formula (11). Three characteristic features are visible in all of the simulations: [1] $\alpha = 0$ at the horizon $r = r_H$, [2] α has a maximum very close to the location of the circular light ray at $r_{\text{ph}} = (3/2)r_H$, [3] for large radii $r \gg r_H$, α is much smaller than in the plunging region. The plunging region is located between the sonic radius r_S and the horizon r_H and is highlighted by the grey colour (r_S is taken from [L19](#)). All lines are normalised by their respective maxima: $\alpha_{\text{max}} = 0.8$ for [L19](#), 0.3 for [P13](#), and 0.3 for [R25](#). Since [R25](#) uses only the Maxwell stress in the local fluid frame (see Section 3), their α definition is mostly valid in the highly magnetised plunging region and we therefore only show [R25](#) data up to r_{ISCO} .

The first term in (11) dominates near to the black hole and far away it tends to zero. The second term dominates far away; it is introduced in order to reflect the asymptotic behaviour of α at large radii.

3. Stress calculated from GRMHD simulations

3.1. General remarks

In the GRMHD simulations of black hole accretion discs one usually assumes that the total stress-energy tensor is the sum of the Reynolds and Maxwell components,⁵

$$T_{\mu\nu}^{\text{Tot}} = T_{\mu\nu}^{\text{Rey}} + T_{\mu\nu}^{\text{Max}}, \quad (14)$$

$$T_{\mu\nu}^{\text{Rey}} = \varepsilon u_\mu u_\nu + p_{\text{gas}} g_{\mu\nu}, \quad (15)$$

$$T_{\mu\nu}^{\text{Max}} = b^2 u_\mu u_\nu + \frac{1}{2} b^2 g_{\mu\nu} - b_\mu b_\nu. \quad (16)$$

The four velocity of matter is

$$u^\mu = \frac{dx^\mu}{ds} = \{u^t, u^r, u^\theta, u^\phi\} \quad (17)$$

and $\varepsilon = \rho + u_{\text{int}} + p_{\text{gas}}$ is the total mass-energy density, with ρ , u_{int} , and p_{gas} being the matter density, internal energy, and pressure, and b^μ is the magnetic field four-vector. In the simulations, one solves the conservation equation

$$\nabla^\mu T_{\mu\nu}^{\text{Tot}} = 0 \quad (18)$$

⁵ We set here $G = c = M = 1$ for simplicity.

together with the material equations (equation of state), the induction equation for the magnetic field, and proper boundary conditions on the chosen metric background that defines the covariant derivative ∇^μ . The continuity equation

$$\nabla_\mu (u^\mu \rho) = 0 \quad (19)$$

assures that matter is neither created nor destroyed during accretion.

The three simulations, [L19](#), [P13](#), and [R25](#), mentioned in the present paper, were performed for accretion onto a non-rotating black hole described by the Schwarzschild metric, with $M = 10 M_\odot$ for [L19](#) (the other two used non-radiative GRMHD, which is scale-free). All are three-dimensional, [P13](#), and [R25](#) use an initial torus threaded by magnetic loops with opposite polarity, and the same prescription for cooling, substituting the radiative losses ([Penna et al. 2010](#)). Unfortunately, both of these simulations are rather short, with a total duration about $20\,000 GM/c^3$, and the time-averaged properties, including α , are only averaged over $5\,000 GM/c^3$ for [R25](#) and $13\,000 GM/c^3$ for [P13](#). During this short duration, the mass accretion rate is barely stable inside the averaging window. [L19](#), on the other hand, is evolved for more than $80\,000 GM/c^3$ and averaged over the last $17\,000 GM/c^3$, with a stable mass accretion rate. This mainly affects the radial extent of a converged region of the simulations, which in the case of the short simulations covers only a few units of r_H above the radius r_{ISCO} .

In contrast to the other two simulations, the puffy disc ([L19](#)) uses *radiative* GRMHD, where the gas conservatively exchanges energy and momentum with a frequency-integrated radiation field, a significantly more realistic approach. The non-radiative simulations use a cooling function to keep the accretion disc geometrically thin; thus, they omit radiation pressure, a crucial component for modelling the disc, and make a strong assumption about its structure.

The behaviour of the stress depends on local and quasi-local effects of the MRI turbulence and on the global constraints given by the black hole geometry. It is natural to think that the local effects are best described in the reference frame comoving with matter $e^\mu_{(k)}$ and the global constraints in the static reference frame attached to the space-time geometry $\tau^\mu_{[k]}$ (see [Kulkarni et al. 2011](#), for the full formulation of this tetrad). The symbols $e^i_{(k)}$ and $\tau^i_{[k]}$ denote an orthonormal base of four-vectors:

$$e^\mu_{(t)} = \langle u^\mu \rangle, \quad \tau^\mu_{[t]} = n^\mu, \quad (20)$$

where $\langle u^\mu \rangle$ is time-averaged matter four-velocity (turbulence is smoothed in time and space) and $n^\mu = \eta^\mu [(\eta\eta)]^{-1/2}$ is the four velocity of the static observer (in the Schwarzschild case). An invariant formula for the stress adopted in [L19](#) and [P13](#) reads

$$\mathbb{T} = \langle T_{\mu\nu} \rangle e^\mu_{(r)} e^\nu_{(\phi)} = \langle T_{(r)(\phi)} \rangle. \quad (21)$$

(the physical meaning of this is explained in [P13](#)). [R25](#), on the other hand, uses only the Maxwell stress in the local fluid frame, defined by the instantaneous fluid velocity, for the calculation of α .

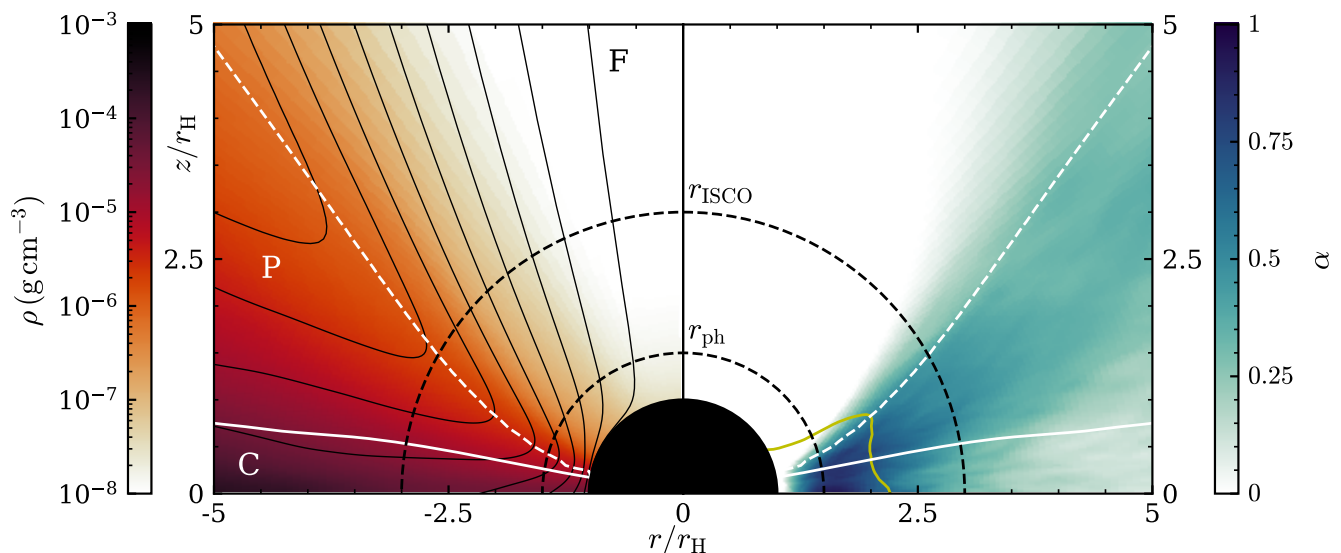


Fig. 2. The structure of a puffy disc consists of three regions: C: dense core, P: puffy region, and F: funnel. *Left:* The colour map of gas density with the magnetic field lines. *Right:* Viscous α colour map, and the magnetosonic surface (yellow contour). In both panels, the white dashed line indicates the photosphere, and the full line indicates the density scale height.

3.2. The puffy discs

The puffy accretion discs are mildly sub- and around-Eddington, radiation pressure-dominated discs around a stellar-mass non-rotating black hole, modelled using 3-dimensional global radiative GRMHD simulations (L19; Sądowski 2016). The simulations were performed using the KORAL code (Sądowski et al. 2013), and were designed so that the accretion disc self-consistently develops from a dense torus acting as a source of matter far from the central black hole. The simulated disc achieved the mass accretion rate $\dot{m} = 0.6 \dot{M}_{\text{Edd}}$. The numerical methods and details of the puffy disc model can be found in Lančová et al. (2026).

The puffy disc is stabilised against thermal instabilities, which are known to be critical in analytical radiation-pressure-dominated accretion discs, by a vertical net flux of magnetic field (Sądowski 2016; Oda et al. 2009; Mishra et al. 2022). The resulting disc is, however, geometrically much thicker than any prediction of the standard models allow, and so its observable properties are distinct from the widely-used accretion disc models (Wielgus et al. 2022).

The structure of the disc, as shown in the left panel of Figure 2, can be separated into two optically thick regions – the geometrically thin dense core (C) and the puffy region (P), surrounded by an optically thin funnel (F) dominated by outflow. The core is defined by the scale-height, which is significantly different from the photosphere height, which encloses the puffy region. The photospheric height of the disc is comparable to the radial distance from the centre ($H/r \sim 1$), whereas the standard disc models predict $H/r < 0.3$ for the same mass accretion rate. The puffy disc structure resembles a thin disc surrounded by a warm corona (Różańska et al. 2015; Gronkiewicz & Różańska 2020). However, the puffy region also supplies most of the mass accretion, in comparison with the very low inflow in the central core.

Figure 2 shows the time and azimuth-averaged structure of the puffy disc. The left panel shows the gas density in colours, the magnetic field lines in black contours, and labels of the three regions. The right panel shows the 2D map of α , where the increase inside the plunging region is apparent – the yellow contour shows magnetosonic surface, that defines the approximate separation between the plunging region and the rotating disc, which we use as r_S in this work. For details of the calculations, see Lančová et al. (2026).

3.3. The puffy discs stress calculations

In extracting α from results of the GRMHD simulations, L19 followed the method described in P13 to calculate the stress, which consists of three steps. First one defines the averaged (in time and azimuth) four velocity $\langle u^\mu \rangle = U^\mu$. Then, one constructs the co-moving tetrad $e^\nu_{(k)}$. Finally, one calculates the total stress and its Reynolds and Maxwell parts, as the tetrad $(r)(\phi)$ components of the corresponding averaged stress-energy tensors $\langle T_{\mu\nu}^{\text{Tot}} \rangle$, $\langle T_{\mu\nu}^{\text{Rey}} \rangle$, $\langle T_{\mu\nu}^{\text{Max}} \rangle$, according to equation (21). The three components of the stress are shown in Figure 3. In both L19 and P13,

$$\alpha = \frac{\mathbb{T}}{p}. \quad (22)$$

However, L19 included the gas, magnetic, and radiation pressures for the α calculations, $p = p_{\text{gas}} + p_{\text{mag}} + p_{\text{rad}}$. This is in contrast with P13, who used only the magnetic and gas pressures, $p = p_{\text{gas}} + p_{\text{mag}}$, since their simulations do not provide the radiation pressure component. R25 further used only the instantaneous fluid-frame Maxwell stress and gas and magnetic pressure.

4. Discussion and future work

In this paper, we report that the results of GRMHD simulations of the black hole accretion disc obtained in several

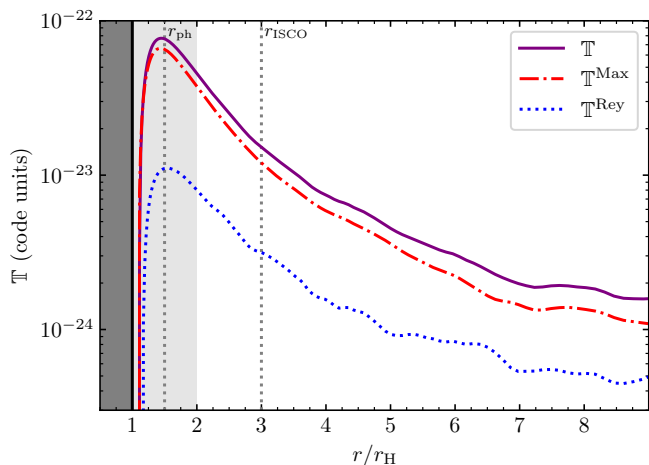


Fig. 3. Behaviour of the total stress $\mathbb{T} = \mathbb{T}^{\text{Max}} + \mathbb{T}^{\text{Rey}}$ and its Reynolds and Maxwell components (the lines shown are taken from L19): the stress is zero at the horizon, it has a maximum at the circular photon orbit and is much smaller far away than in the plunging region. The behaviour of the stress is remarkably similar to the behaviour of the inverse of the square of the “gyration radius” \tilde{r} .

independent studies by different authors seem to indicate a universal radial dependence of the Shakura-Sunyaev α -viscosity coefficient, which most probably reflects fundamental properties of the stress itself. This finding suggests two directions of future research: First, an explanation from first principles of the universal stress behaviour seen in Figure 3, and second, an application of our α -viscosity formula (11) to construct semi-analytic models of thin and slim discs.

4.1. Fundamental stress properties

We will discuss fundamental physical reasons for such behaviour in a forthcoming, much more mathematically minded publication. In this subsection, we only briefly hint at some relevant points, appealing to physical intuition rather than giving solid mathematical proofs. One of the issues that we will carefully clarify (because it is often a source of confusion) is that: the stress is zero at the horizon, yet the equivalence principle assures that one cannot know from local measurements about the horizon crossing. Or, in a wider context — the MRI builds the stress locally, in the comoving frame, but some of the stress properties reflect the global assets of the black hole space-time.

4.1.1. Stress is zero at the horizon

Let us cast equation (2) in the form

$$\mathbb{T} = \dot{J} - \langle \dot{M} \rangle \langle j \rangle \quad (23)$$

that underlines the physical meaning of the stress: it represents the part of the angular momentum flux through a surface \mathcal{S} that is not carried with the mean mass accretion flux $\langle \dot{M} \rangle \langle j \rangle$. Here $\langle j \rangle$ is the mean specific angular momentum at \mathcal{S} . Abramowicz et al. (2010) applied (23) and argued that when a sphere \mathcal{S} of radius r in an accretion disc is crossed by a “mean” accretion flow $\langle \dot{M} \rangle$ in the + direction (towards

the black hole), turbulence causes an additional (fluctuating) downstream flux $\delta \dot{M}^+$ and an upstream flux $\delta \dot{M}^-$, and therefore the total fluxes of mass in the + and - directions are $\dot{M}^+ = \langle \dot{M} \rangle + \delta \dot{M}^+$ and $\dot{M}^- = \delta \dot{M}^-$. Therefore,

$$\mathbb{T} = \frac{1}{2}(\delta \dot{M}^-)(\delta j), \quad (24)$$

where $(\delta j) = [\dot{M}^+ j^+ - \dot{M}^- j^-] / \langle \dot{M} \rangle$.

From equation (24), Abramowicz et al. (2010) have deduced that, if the surface \mathcal{S} coincides with the black hole horizon, then no upstream flux of mass exists, ($\delta \dot{M}^- = 0$) and hence, there is no stress at $r = r_H$. This simple argument, which captures the essence of the relevant physics, was later extended by Lasota et al. (2014) who considered an arbitrary stress-energy tensor $T_{\mu\nu}$, that describes any kind of matter or field, in particular the electromagnetic field. Specifically, for the electromagnetic field in the GRMHD environment, Lasota et al. (2014) rigorously proved that the Blandford-Znajek mechanism is an electromagnetic version of the Penrose process. They showed that, although angular momentum is transported along the field lines of a strongly enhanced magnetic field, no magnetic stress (torque) is exerted at the horizon. Instead, the black hole absorbs negative energy and negative angular momentum, resulting in a reduction of its rotational energy. As a particular example, Lasota et al. (2014) showed that this general principle (“no stress but negative energy absorption”) takes place in magnetically arrested accretion discs (Bisnovatyi-Kogan & Ruzmaikin 1974; Narayan et al. 2003).

4.1.2. Stress has its maximum at the photon radius

Figure 3 shows that GRMHD simulations clearly indicate that both the Reynolds and the Maxwell components of the stress (and therefore also the total stress) peak up sharply at the location of the radius of the circular photon orbit. In a forthcoming analytic study we plan to address the question of whether the stress maximum is caused by the reversal of the sense of *outward* and *inward* radial directions that is known to occur at the location of the circular photon orbit $r_{\text{ph}} = (3/2)r_H$. For $r < r_{\text{ph}}$, “out” points towards the black hole at the centre (Abramowicz et al. 1995; Abramowicz & Prasanna 1990). The reversal influences all of the dynamical properties of rotation, in particular the reversed Rayleigh criterion demands that, for stability, angular momentum should *increase inwards*, meaning towards the black hole. Correspondingly, the Rayleigh stress transports angular momentum *inwards*, into the black hole (Anderson & Lemos 1988). There are several other examples of this reversal described in a popular Scientific American article by Abramowicz (1993).

4.1.3. At large radii $\alpha = (\text{shear})/(\text{vorticity})$

In the far region $r \gg r_H$

$$\alpha \approx \alpha_\infty = \text{const}, \quad (25)$$

with $10^{-2} \lesssim \alpha_\infty \lesssim 10^{-1}$. Abramowicz et al. (1996) noticed that in the far region, for flows that are dominated by matter spiralling down along orbits that may be considered almost circular, a more detailed fitting is consistent with

$$\alpha \approx \frac{\alpha_\infty}{3} \left(\frac{\sigma}{\omega} \right), \quad (26)$$

where the kinematic invariants shear = σ and vorticity = ω are given in the Schwarzschild space-time by

$$\sigma^2 = -\frac{1}{4}(1 - \Omega j)^{-2}(\tilde{r})^{+2}(\nabla^\mu \Omega)(\nabla_\mu \Omega), \quad (27)$$

$$\omega^2 = -\frac{1}{4}(1 - \Omega j)^{-2}(\tilde{r})^{-2}(\nabla^\mu j)(\nabla_\mu j). \quad (28)$$

This possibly reflects the origin of the stress as driven by the *local* magnetorotational instability (MRI; Balbus & Hawley 1991), with turbulence being sensitive to local gradients of angular velocity Ω and specific angular momentum j .

The numerical results of Abramowicz et al. (1996) for stratified MRI turbulence were verified by Hawley et al. (1999), who considered unstratified MRI turbulence for a fine mesh of shear parameters q . In their local shearing box simulations, $q = -d \ln \Omega / d \ln r$ is the double-logarithmic angular velocity gradient, which quantifies the strain of the background velocity Ω_0 , $\sigma = q\Omega_0/\sqrt{2}$. By contrast, the vorticity of the background velocity is $\omega = r^{-1}d(r^2\Omega/dr)/\sqrt{2} = (2 - q)\Omega_0/\sqrt{2}$. Hawley et al. (1999) noted that for small values of q , the turbulent fluctuations in the stress are dominated by the magnetic contributions. Interestingly, based on their analytical considerations, they also pointed out that the magnetic stress fluctuations couple directly to the strain $\sigma \propto q$, while the kinetic stress fluctuations couple to the vorticity $\omega \propto 2 - q$. Therefore, $\sigma/\omega = q/(2 - q)$, so for small values of q , the vorticity $\omega \propto 2 - q$ limits the turbulent transport quantified by α , while strain $\sigma \propto q$ promotes it.

These results were subsequently corroborated by Pessah et al. (2006, 2008) using a linear stability analysis. In particular, they confirmed the observation that the turbulent stresses are not simply proportional to the local shear, as one might have naively expected. Similar conclusions were also drawn by Liljeström et al. (2009) using a closure model of Ogilvie (2003). The numerical results of Abramowicz et al. (1996) and Hawley et al. (1999) were later also confirmed for much taller boxes of up to eight scale heights (Nauman & Blackman 2015).

5. Conclusions

We have suggested an improvement to the famous, analytic, Shakura-Sunyaev α -prescriptions for the stress $\mathbb{T} = \alpha p$. Instead of the original ansatz $\alpha = \text{const}$, we propose

$$\alpha = \alpha_P (r_H/\tilde{r})^2 + \alpha_\infty (\eta\eta), \quad \tilde{r}^2 = -\frac{(\xi\xi)}{(\eta\eta)}, \quad (29)$$

with $\alpha_P \sim 1$, $\alpha_\infty \sim 0.01$ being phenomenological constants and $r_H = 2GM/c^2$ being the black hole horizon radius. This analytic formula is based on the results of GRMHD simulations that describe black hole accretion discs with sub-Eddington and around-Eddington accretion rates. It is analytic and expressed in terms of coordinate-independent quantities — the Kerr metric Killing vectors η^μ , ξ^μ . It is short, simple, and explicit in any specific coordinates used in the black hole accretion studies. It accurately embraces fundamental properties of the stress in the curved black hole space-time: the stress is zero at the event horizon, it is smaller far away from the black hole than in the plunging region closer to it, and it peaks up near the location of the circular light radius.

We plan to use (29) to calculate improved models of both stationary and non-stationary slim accretion discs. For the stationary ones, we will first need to convert the equations given by Sądowski (2009) into the comoving frame so as to ensure that the stress description (29) corresponds directly to that used in L19 and other GRMHD simulations. For the non-stationary ones, the simulations by Szuszkiewicz & Miller (1998) and Szuszkiewicz & Miller (2001) have already been performed in a Lagrangian frame, as is optimal for various reasons. Further work will involve applying (29) into a similar scheme but with modifications to give an improved relativistic treatment of the accretion flow between the sonic radius and the black hole horizon, enabling it to follow the essential characteristics of the flow there. This approach should make it possible to calculate a long time evolution of the disc, as before, which is crucial for understanding the observational appearance of objects powered by accretion onto black holes.

The most exciting research outcome that one may anticipate from the findings of this paper is the possibility of explaining these features of the stress:

$$\mathbb{T}(r_H) = 0, \quad \mathbb{T}(r_{\text{ph}}) = \mathbb{T}_{\text{max}}, \quad \mathbb{T}(r \gg r_H) \propto \sigma/\omega,$$

which may reflect the way in which the quasi-local MRI turbulence interacts with the global constraints coming from the space-time geometry of the black hole.

Acknowledgements. The first version of this draft was prepared at the RAGtime workshop in Opava. MA and JH acknowledge the Czech Science Foundation (GAČR) grant No. 21-06825X, and DL project No. 25-16928O and the internal grant of the Silesian University SGS/25/2024. AB acknowledges support by the Swedish Research Council (Vetenskapsrådet) under grant No. 2025-05957. JM acknowledges continuing support from the Italian Istituto Nazionale Previdenza Sociale and provision of facilities by the University of Oxford; MW is supported by a Ramón y Cajal grant RYC2023-042988-I from the Spanish Ministry of Science and Innovation and acknowledges financial support from the Severo Ochoa grant CEX2021-001131-S funded by MCIN/AEI/ 10.13039/501100011033. This work was supported by the Ministry of Education, Youth and Sports of the Czech Republic through the e-INFRA CZ (ID:90254).

Data availability. The simulation data underlying this article are available upon reasonable request to the corresponding authors.

References

- Abramowicz, M., Brandenburg, A., & Lasota, J.-P. 1996, MNRAS, 281, L21
- Abramowicz, M. A. 1993, Scientific American, 268, 74
- Abramowicz, M. A., Czerny, B., Lasota, J. P., & Szuszkiewicz, E. 1988, ApJ, 332, 646
- Abramowicz, M. A., Jaroszyński, M., Kato, S., et al. 2010, A&A, 521, A15
- Abramowicz, M. A., Miller, J. C., & Stuchlík, Z. 1993, Phys. Rev. D, 47, 1440
- Abramowicz, M. A., Nurowski, P., & Wex, N. 1995, Classical and Quantum Gravity, 12, 1467
- Abramowicz, M. A. & Prasanna, A. R. 1990, MNRAS, 245, 720
- Anderson, M. R. & Lemos, J. P. S. 1988, MNRAS, 233, 489
- Balbus, S. A. & Hawley, J. F. 1991, ApJ, 376, 214
- Bisnovatyi-Kogan, G. S. & Ruzmaikin, A. A. 1974, Ap&SS, 28, 45
- Gronkiewicz, D. & Różańska, A. 2020, A&A, 633, A35
- Hawley, J. F., Balbus, S. A., & Winters, W. F. 1999, ApJ, 518, 394
- Kulkarni, A. K., Penna, R. F., Shcherbakov, R. V., et al. 2011, MNRAS, 414, 1183
- Lančová, D., Abarca, D., Kluźniak, W., et al. 2019, ApJ, 884, L37
- Lančová, D., Wielgus, M., Abramowicz, M., et al. 2026, in preparation
- Lasota, J.-P., Gourgoulhon, E., Abramowicz, M., Tchekhovskoy, A., & Narayan, R. 2014, Phys. Rev. D, 89, 024041
- Liljeström, A. J., Korpi, M. J., Käpylä, P. J., Brandenburg, A., & Lyra, W. 2009, Astronomische Nachrichten, 330, 92

- Mishra, B., Fragile, P. C., Anderson, J., et al. 2022, *ApJ*, 939, 31
- Narayan, R., Igumenshchev, I. V., & Abramowicz, M. A. 2003, *PASJ*, 55, L69
- Nauman, F. & Blackman, E. G. 2015, *MNRAS*, 446, 2102
- Novikov, I. D. & Thorne, K. S. 1973, in *Black Holes (Les Astres Occlus)*, ed. C. Dewitt & B. S. Dewitt, 343–450
- Oda, H., Machida, M., Nakamura, K. E., & Matsumoto, R. 2009, *ApJ*, 697, 16
- Ogilvie, G. I. 2003, *MNRAS*, 340, 969
- Penna, R. F., McKinney, J. C., Narayan, R., et al. 2010, *MNRAS*, 408, 752
- Penna, R. F., Sądowski, A., Kulkarni, A. K., & Narayan, R. 2013, *MNRAS*, 428, 2255
- Pessah, M. E., Chan, C.-K., & Psaltis, D. 2006, *Phys. Rev. Lett.*, 97, 221103
- Pessah, M. E., Chan, C.-K., & Psaltis, D. 2008, *MNRAS*, 383, 683
- Różańska, A., Malzac, J., Belmont, R., Czerny, B., & Petrucci, P.-O. 2015, *A&A*, 580, A77
- Rule, J., Mummery, A., Balbus, S., Stone, J. M., & Zhang, L. 2025, *MNRAS*, 542, 377
- Shakura, N. I. & Sunyaev, R. A. 1973, *A&A*, 24, 337
- Sądowski, A. 2009, *ApJS*, 183, 171
- Sądowski, A. 2016, *MNRAS*, 459, 4397
- Sądowski, A., Narayan, R., Tchekhovskoy, A., & Zhu, Y. 2013, *MNRAS*, 429, 3533
- Szuskiewicz, E. & Miller, J. C. 1998, *MNRAS*, 298, 888
- Szuskiewicz, E. & Miller, J. C. 2001, *MNRAS*, 328, 36
- Wielgus, M., Lančová, D., Straub, O., et al. 2022, *MNRAS*, 514, 780

Appendix A: Kerr metric formulae

The covariant definitions of the quantities used in the paper are given in terms of Kerr metric symmetry generators: the Killing vector of time symmetry η^i and the Killing vector of axial symmetry ξ^i . The Killing vectors obey

$$\nabla_{(i}\eta_{k)} = 0, \quad \nabla_{(i}\xi_{k)} = 0, \quad \eta^i \nabla_i \xi_k = \xi^i \nabla_i \eta_k. \quad (\text{A.1})$$

The frame dragging ω and the gravity potential Φ obey

$$\omega = -\frac{(\eta\xi)}{(\xi\xi)}, \quad \Phi = -\frac{1}{2} \ln[(\eta\eta) + 2\omega(\eta\xi) + \omega^2(\xi\xi)] \quad (\text{A.2})$$

which help to define the four-velocity of the stationary observer (ZAMO)

$$n^i = e^\Phi(\eta^i + \omega\xi^i), \quad (nn) = 1. \quad (\text{A.3})$$

A circular motion at the equatorial plane symmetry of the Kerr metric is defined by writing two equivalent expressions for the four velocity of matter,

$$u^i = A(\eta^i + \Omega\xi^i), \quad A^{-2} = (\eta\eta) + 2\Omega(\eta\xi) + \Omega^2(\xi\xi), \quad (\text{A.4})$$

$$u^i = \gamma(n^i + v\tau^i), \quad \tau^i = \xi^i/r, \quad r^2 = -(\xi\xi). \quad (\text{A.5})$$

These equations invariantly define the angular velocity Ω , the orbital velocity v and the redshift factor $\gamma^{-2} = 1 - v^2$. The specific angular momentum j obeys

$$j = -\frac{(u\xi)}{(u\eta)}, \quad j = v\tilde{r} = \tilde{\Omega}\tilde{r}^2, \quad (\text{A.6})$$

where $\tilde{\Omega} = \Omega - \omega$ and

$$\tilde{r} = re^\Phi \quad (\text{A.7})$$

is the gyration radius; see [Abramowicz et al. \(1995\)](#) for more details.